ISSN 2228-9860 eISSN 1906-9642 CODEN: ITJEA8

International Transaction Journal of Engineering, Management, & Applied Sciences & Technologies

http://TuEngr.com

Impacts of Temperature on the Silicate Scale Severity and Morphologies Studies

Rozana Azrina Sazali[1*], Noor Shamimi Ramli[1], Ken Sorbie[2], Lorraine Boak[2]

[1] *Department of Oil and Gas Engineering, School of Chemical Engineering, College of Engineering, Universiti Teknologi MARA, MALAYSIA.*

[2] *Flow Assurance and Scale Team (FAST), School of Energy, Geoscience, Infrastructure and Society (EGIS), Heriot-Watt University, UNITED KINGDOM.*

**Corresponding Author (Tel: +60-355436416, Email: rozana592@uitm.edu.my).*

Paper ID: 12A9R

Volume 12 Issue 9

Received 19 April 2021
Received in revised form 01 July 2021
Accepted 07 July 2021
Available online 14 July 2021

Keywords:
Oilfield Scale; Alkaline Surfactant Polymer Flooding (ASP); Silicate Scaling Build up; Precipitates Analysis; Silicate Scaling Mechanism; Flow Assurance; Petroleum Production.

Abstract

ASP flooding is one of the most promising and cost-effective Chemical Enhanced Oil Recovery (CEOR) methods. Nevertheless, it faces the problem of causing severe silicate scale formation in sandstone reservoirs. As the ASP chemical package is injected and progresses towards the production well, the alkali reacts with the formation of water and rock minerals which trigger the increase of the scaling ions concentration (Ca^{2+}, CO_3^{2-}, SiO_2^{3-}) within the system. As the production fluid moves into or near the well, changes in pressure and temperature will be encountered resulting in silicate scale formation in the perforations, casing, tubing, and surface facilities. This study was conducted to determine how temperature affected the severity of silicate scales and the morphology of silicate scales produced as well as the effect of different Mg/Ca stoichiometric ratios. In these experiments, the silicate scale was reproduced by allowing the reaction of magnesium and calcium (to represent the formation water), and silicate ions (to represent the ASP slug) for 22 hours at room temperature/ 60°C/ 90°C at a constant pH of 8.5 and ambient pressure. Visual inspection of the formation of precipitates was carried out. The filtrate was analysed by AAS and the corresponding precipitates were analysed using FTIR, XRF, and XRD techniques.

Disciplinary: Chemical and Petroleum Engineering.

Cite This Article:

Sazali, R.A., Ramli, N., Sorbie, K.S., and Boak, L.S. (2021). Impacts of Temperature on the Silicate Scale Morphologies Studies and Severity. *International Transaction Journal of Engineering, Management, & Applied Sciences & Technologies, 12*(9), 12A9R, 1-16. http://TUENGR.COM/V12/12A9R.pdf DOI: 10.14456/ITJEMAST.2021.186

1 Introduction

Production from an oil reservoir, either by a conventional primary or a secondary extraction technique, is only expected to produce about 20-40% of the original oil in place (OOIP), leaving

significant quantities of oil in the reservoir (Nurxat et al., 2015). In other words, it is the usual practice to assume that a reservoir will successfully produce only a fraction of the OOIP. The application of the EOR technique in mature oilfields may be an attractive solution towards remedying this low level of recovery (Babadagli, 2007).

ASP flooding has been reported as being able to improve oil recovery incrementally compared to waterflooding by up to 20%. The intention in applying ASP is to improve the displacement efficiency and to expand sweep efficiency by injecting polymer, surfactant, and alkali at the same time. Guo et al. (2017) reported that the ASP flooding field in Daqing, China successfully produced 3.5 million tons which accounted for nine percent of total oil production in the field for the year 2015. They also reported there were 22 ASP flooding industrial blocks in Daqing, covering 7231 injectors and producers in 2016.

However, a key problem of ASP is the excessive formation of silicate scale in sandstone reservoirs which are composed of several minerals primarily silica (Gunnarsson & Arnórsson, 2003).

2 Literature Review

Alkali reacts with formation water and rock minerals during ASP flooding and this will trigger the increase of the concentrations of the scaling ions (Ca^{2+}, CO_3^{2-}, SiO_2^{3-}) within the system. As these fluids move into or near the production well, pressure, temperature, brine mixing, and pH changes the result in silicate scale deposition (Umar & Saaid, 2013).

Alkali reacts with the silica in the rock formation which dissolves to produce silicic acid $H_4Si(OH)_4$ (Amjad & Zuhl, 2009). This silicic acid will then be ionized to monomeric silica in the solution before it turns into reactive silica. The hydroxide ion (OH^-), acting as a catalyst, promotes the ionization of dissolved silica and colloidal silica will be formed from the polymerization of reactive silica. This colloidal silica may then form an amorphous silica scale, and will also tend to form a metallic silicate scale in the presence of metal ions such as Mg^{2+} (Mahat et al., 2016).

Silica (SiO_2) scaling is observed in nearly all geothermal systems (Jing et al., 2013). The silica may be produced by several pathways depending on the temperature of the brine. Amorphous silica accumulation occurs at low temperatures. The deposition of minerals is regulated by their solubility at the highest temperatures. However, the rate of silica deposition/dissolution is a function of both the degree of supersaturation and temperature (Oddo et al., 1991).

Mg^{2+} ions, if present, may interact with particles of colloidal silicate and form an amorphous silicate of magnesium. After water softening, the presence of any residual magnesium will precipitate in the ASP as $Mg(OH)_2$. Then magnesium may be introduced into the connate water of neutral pH. According to Umar and Saaid (2013), the solubility of magnesium will increase with an increase in temperature. The colloidal silicate particles can keep growing and form amorphous silica scales, even in the absence of divalent cations.

The high pH of the ASP water in the presence of the calcium ion mixing in the well will also encourage the formation of calcium carbonate scale. This calcite scale formation may provide

nuclei for the further formation of silicate scales (Gill, 1998). $CaCO_3$ scale becomes more insoluble at higher temperatures, and thus a solution at equilibrium with $CaCO_3$ will precipitate more solid as the temperature is increased. The tendency to form $CaCO_3$ also increases with the increase of pH, as the solution becomes less acidic. At this high pH condition, it is believed that the calcium (Ca^{2+}) and magnesium (Mg^{2+}) ions will further be reacted with carbonate (CO_3^{2-}) or hydroxide (OH^-) where this will serve as nuclei that catalyse the silicate scale precipitation (Sonne et al., 2012).

Various crystalline and amorphous types of silica may form depending on the conditions. Crystalline silica has water solubility that is very low with 6 mgL^{-1} SiO_2. On the other hand, amorphous silica has a much higher solubility in the range of 100 to 140 mgL^{-1} SiO_2. Silica scaling probability increases when the levels of silica dissolve in an aqueous system that exceeds the limit of amorphous silica solubility at ambient temperature in the range of 120-140 mgL^{-1} (Brown, 2011).

In the oil and gas industry, silicate scale formation in the perforation channels, casing surface, tubing, and surface facilities can be a very serious problem, resulting in significant loss of production (Jing et al., 2013). Therefore, this study was i) to investigate how temperature affects the silicate scale deposition; ii) to determine the morphology of silicate scales produced; and iii) to examine the effect of varying Mg/Ca stoichiometric ratios on the silicate scale formation.

3 Method

The test of silicate scaling was carried out by allowing the reaction of magnesium and/or calcium with silicate ions for 22 hours. Tests were carried out at room temperature (25°C), 60°C, and 90°C at a constant pH of 8.5 and ambient pressure.

Silicate brine containing silicon at a concentration of 1880 ppm, representing a possible ASP slug, was prepared. To represent formation water, a brine containing 1800 ppm magnesium and calcium ions was prepared separately. The solution was filtered before use using 0.45 microns filter paper. The initial pH of the individual brines was measured.

At each of 25°C, 60°C, and 90°C, 7 different mixed brine solutions at various ion concentrations were tested (each case was prepared in duplicate), see Table 1. The mixed brines, noted as numbers 5 to 7 in Table 1, were used to investigate the effect of different calcium to magnesium molar ratios on the occurrence of silicate scaling. 187.5ppm, 375ppm and 750ppm Ca were chosen to represent the initial Ca:Mg molar ratio of 0.25, 0.5, and 1, respectively. The exact composition of the mixed brine used in each test condition is presented in Tables 2, 3, and 4.

Table 1: Final Mixed Brine Concentration

Experiment	Final Mix Concentration (ppm)		
	Silicon	Magnesium	Calcium
1 (Si only)	1880	0	0
2 (Si only)	940	0	0
3 (Si/Mg; Mg in excess)	940	900	0
4 (Si/Ca; Si in excess)	940	0	900
5 (Si/Mg/Ca; Ca:Mg=0.25)	940	450	187.5
6 (Si/Mg/Ca; Ca:Mg=0.5)	940	450	375
7 (Si/Mg/Ca; Ca:Mg=1)	940	450	750

The initial pH of each of the mixed brines was measured and immediately adjusted to pH8.5. The brines were shaken and stirred consistently following a systematic pH adjustment procedure before being placed in the oven and heated to the test temperatures.

Continuous visual inspections of the bottles were made to observe the formation of precipitates. The solution turbidity was observed visually and photographed. The supernatant of each brine was sampled after 2 and 22 hours, respectively, before being analysed by Atomic Absorption Spectrometry (AAS).

The samples were then filtered and the concentration of magnesium, calcium, and silica in the filtrate was analysed using the AAS. This allowed us to determine the amount of magnesium and calcium silicates that had precipitated. The precipitates obtained were then analysed by Fourier-transform infrared spectroscopy (FTIR), X-Ray Diffraction (XRD), and X-ray fluorescence (XRF). The experimental procedure used is shown schematically in Figure 1.

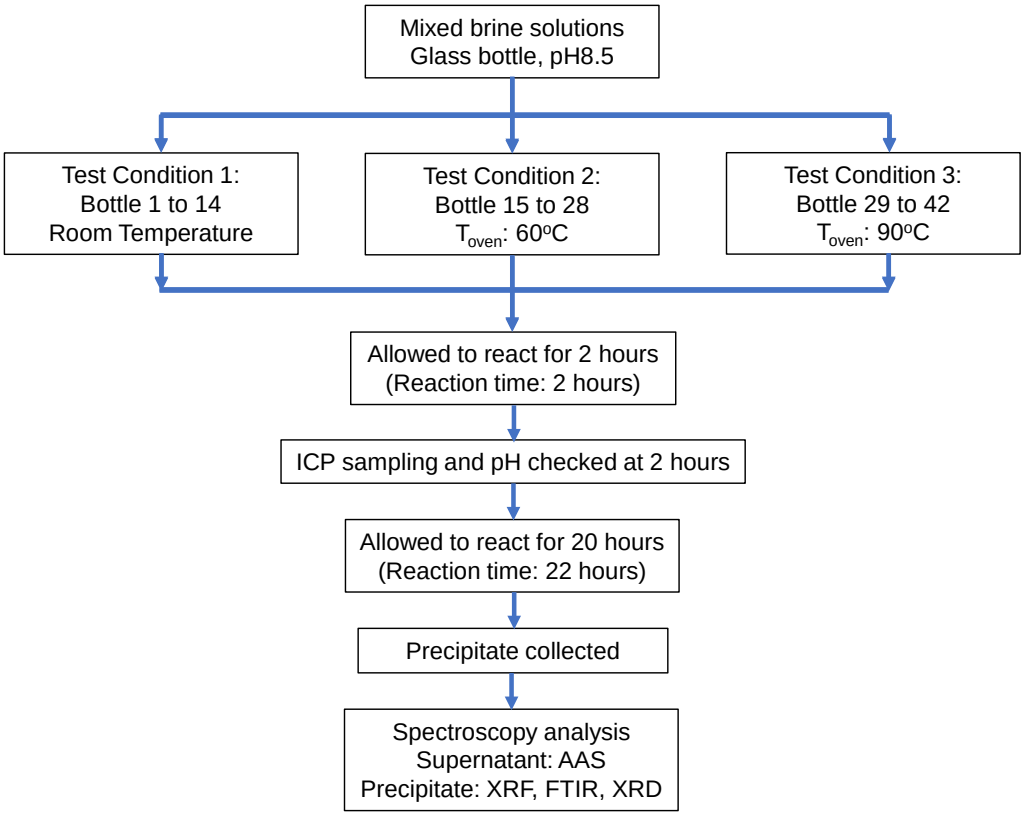

Figure 1: Experimental Procedure for the Effect of Temperature on Silicate Scaling Test

Table 2: List of the Mixed Solution in the Glass Bottle at Test Condition 1 (Room Temperature, pH 8.5)

Experiment	Glass Bottle	Initial Mixed Volume
1	1 & 2	100 ml 1880ppm Si
2	3 & 4	50 ml 1880ppm Si + 50 ml distilled water
3	5 & 6	50 ml 1880ppm Si + 50ml 1800ppm Mg
4	7 & 8	50 ml 1880ppm Si + 50ml 1800ppm Ca
5	9 & 10	50 ml 1880ppm Si + 25ml 1800ppm Mg + 25ml 750ppm Ca
6	11 & 12	50 ml 1880ppm Si + 25ml 1800ppm Mg + 25ml 1500ppm Ca
7	13 & 14	50 ml 1880ppm Si + 25ml 1800ppm Mg + 25ml 3000ppm Ca

Table 3: List of the Mixed Solution in the Glass Bottle at Test Condition 2 (60°C, pH8.5)

Experiment	Glass Bottle	Initial Mixed Volume
1	15 & 16	100 ml 1880ppm Si
2	17 & 18	50 ml 1880ppm Si + 50 ml distilled water
3	19 & 20	50 ml 1880ppm Si + 50ml 1800ppm Mg
4	21 & 22	50 ml 1880ppm Si + 50ml 1800ppm Ca
5	23 & 24	50 ml 1880ppm Si + 25ml 1800ppm Mg + 25ml 750ppm Ca
6	25 & 26	50 ml 1880ppm Si + 25ml 1800ppm Mg + 25ml 1500ppm Ca
7	27 & 28	50 ml 1880ppm Si + 25ml 1800ppm Mg + 25ml 3000ppm Ca

Table 4: List of the Mixed Solution in the Glass Bottle at Test Condition 3 (90°C, pH8.5)

Experiment	Glass Bottle	Initial Mixed Volume
1	29 & 30	100 ml 1880ppm Si
2	31 & 32	50 ml 1880ppm Si + 50 ml distilled water
3	33 & 34	50 ml 1880ppm Si + 50ml 1800ppm Mg
4	35 & 36	50 ml 1880ppm Si + 50ml 1800ppm Ca
5	37 & 38	50 ml 1880ppm Si + 25ml 1800ppm Mg + 25ml 750ppm Ca
6	39 & 40	50 ml 1880ppm Si + 25ml 1800ppm Mg + 25ml 1500ppm Ca
7	41 & 42	50 ml 1880ppm Si + 25ml 1800ppm Mg + 25ml 3000ppm Ca

4 Result and Discussion

The analyses by FTIR, XRD, and XRF were carried out on the precipitates collected after 22 hours, filtered through a 0.2 µm filter paper, and dried in a desiccator for at least 24 hours. The solid samples were then crushed by a mortar which turned them into powder before being analysed. Analysis by AAS was performed on the supernatant of the liquid test samples to determine the ion compositions, particularly of Ca^{2+}, $Mg^{2+,}$ and Si. Supernatant liquid samples were collected at 2 hours and 22 hours and quenched into 1% EDTA/NaOH before being analysed.

4.1 Conditions and Observation

It was observed that under all three conditions, a clear solution without any turbidity can be seen for Si-only solution of 1880ppm Si and 940ppm Si, see Figure 2. As for the other Si/Mg/Ca scaling solution, a cloudy solution appeared as soon as the solutions were mixed (and the pH of the solution was adjusted). In Figure 3, the colloidal solutions were observed to settle to the bottom part of the bottle at different rates.

Figure 2: Physical Observation after 22 hours of reaction time for Si-only containing brine with 1880ppm Si (Left) and 940ppm Si (Right)

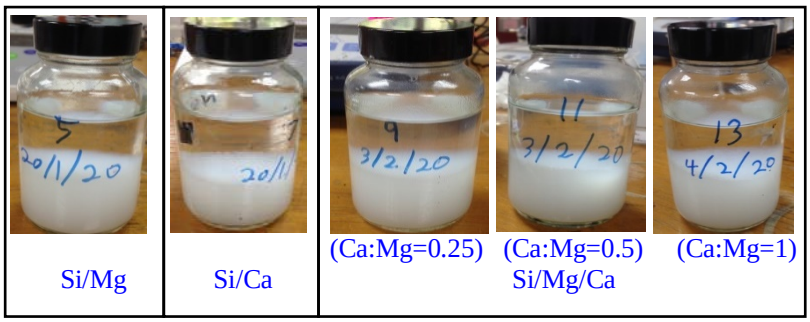

a) T_{Room}

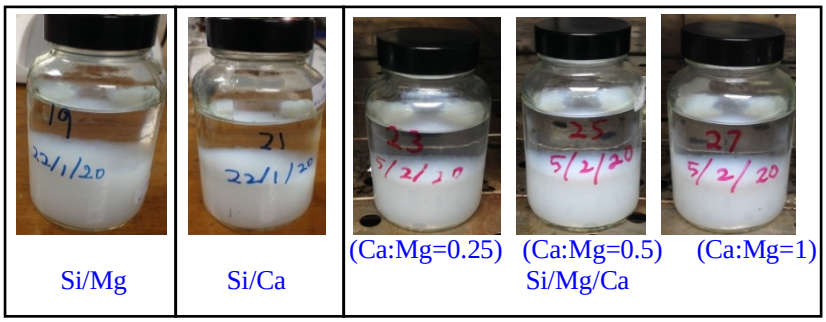

b) T = 60°C

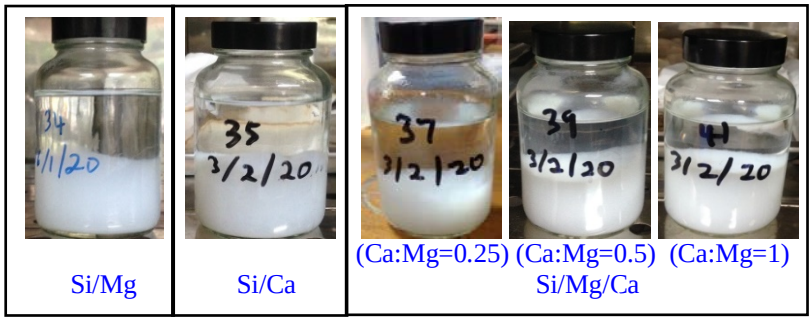

c) T = 90°C

Figure 3: Physical Observation of Si/Mg/Ca Containing Brine with Various Concentrations at T_{room}, 60°C, 90°C at 0 hours i.e. immediately after being mixed and pH adjusted.

4.2 AAS Results: Severity of Silicate Scaling and Extent of Reaction

AAS data showed the amount of magnesium and calcium ions reaction after 2 and 22 hours in the Si/Mg/Ca mixed brines at various temperatures. Figure 4 shows that there were differences in the number of magnesium ions that have reacted under each of the three test conditions i.e. Test Conditions 1, 2, and 3. This may be an indicator of slightly different compounds being formed at each temperature.

It is well known that the reaction mechanism of this silica/silicate scale is very complicated due to its high dependency on the pH value. Silica scale is anticipated in the pH condition of less than 8.5 as opposed to magnesium silicate scale that is aggravated in the pH of higher than 8.5. It was reported elsewhere that the solubility of silica was highly independent of the pH between pH 6 to 8. In addition, the silica scale displayed normal solubility characteristic to a temperature which contrasted with the magnesium silicate scale that exhibited inverse solubility.

Based on Figure 4, it was found that more magnesium ions reacted in 940ppm Si: 900ppm Mg mixed brine for Test Condition 1 (room temperature) than Test Condition 2 (60°C) and Test

Condition 3 (90°C). This may be due to more magnesium ions reacting to form magnesium hydroxide $Mg(OH)_2$, (not the magnesium silicate) at room temperature. The solubility of this $Mg(OH)_2$ increased when the temperature was increased i.e. normal solubility; causing the amount of magnesium ion reacted to decrease at 60°C and 90°C in Test Conditions 2 and 3, respectively.

The solubility of $Mg(OH)_2$ was 0.00064 g/100 mL at 25°C and 0.004 g/100 mL at 100°C. In addition, the number of magnesium ions reacted was also found to increase from the reaction time of 2 hours to 22 hours for all three test conditions.

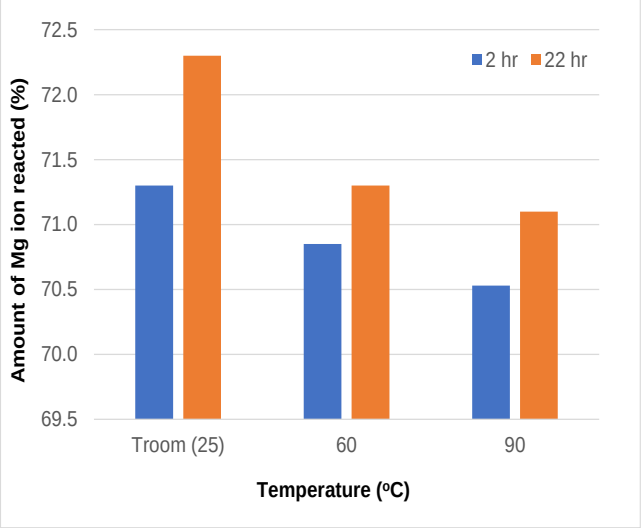

Figure 4: Percentage Amount of Mg Ions Reacted under Different Temperature Conditions for 940ppm Si: 900ppm Mg Scaling Brine

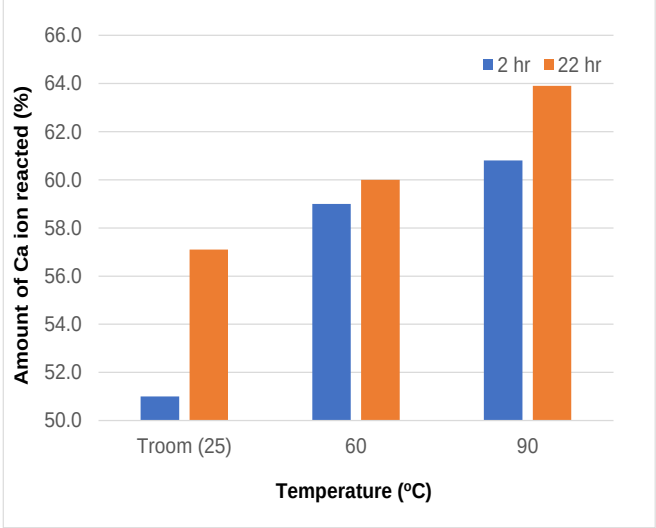

Figure 5: Percentage Amount of Ca Ions Reacted under Different Temperature Conditions for 940ppm Si: 900ppm Mg Scaling Brine

In contrast, the amount of Ca ion reacted was found to be the highest at 90°C as compared to lower temperatures, see Figure 5. The lowest amount of calcium ions reacted in Test Condition 1 was due to the high calcium solubility at low-temperature conditions i.e. calcium silicate is inverse solubility. The number of calcium ions reacted increased when the temperature increased to 60°C and 90°C because of the decrease in calcium silicate solubility as the temperature increased. The same pattern was observed for Ca^{2+} (as for Mg^{2+}), where the percentage of calcium ions reacted was also found to increase from the reaction time of 2 hours to 22 hours in all three test conditions.

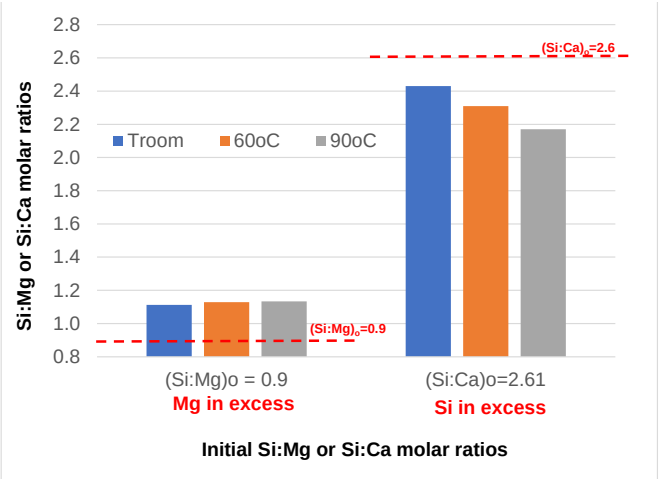

Figure 6: Si:Mg and Si:Ca molar ratios in the precipitates formed in Experiment 3 (940Si:900Mg) & Experiment 4 (940Si:900Ca) at various temperatures

Figure 6 shows the Si:Mg molar ratios and Si:Ca molar ratios in the precipitates formed in both Si/Mg and Si/Ca scaling solutions, respectively. When the Mg was in excess initially as compared to Si ion i.e. $(Si:Mg)_o \approx 0.9$, the resultant Si:Mg molar ratios in the precipitates was approximately 1 at all temperatures. This means, approximately 1 mol of magnesium is bridged to 1 mol of silicon ion.

In contrast, when the Si was in excess in the Si/Ca scaling solution i.e. $(Si:Ca)_o \approx 2.6$; this has resulted in Si:Ca molar ratios of more than 2 in the precipitates formed at all temperatures tested. This may be due to the polymerization of silica that occurred before the calcium ion reacted with the silica backbone. The Si:Ca molar ratios were also found to decrease as temperature increased due to more reaction of calcium with the silica to form the calcium silicate scale.

Figure 7 shows the Ca:Mg molar ratios in the precipitates formed in various initial Ca:Mg molar ratios at all temperatures tested. Generally, the Ca:Mg molar ratios increases with the increasing temperatures at all initial Ca:Mg tested. However, lower molar ratios of Ca:Mg were observed in the precipitates as compared to their initial molar ratios. This indicates that silicates favour Mg ions when both Ca and Mg ions are present. However, it is well known that the solubility of calcium silicate is much higher than that of magnesium silicate and this may explain why silica would first be removed as magnesium silicate. Hence, it is anticipated that calcium silicate may only be formed in the presence of a low concentration of magnesium.

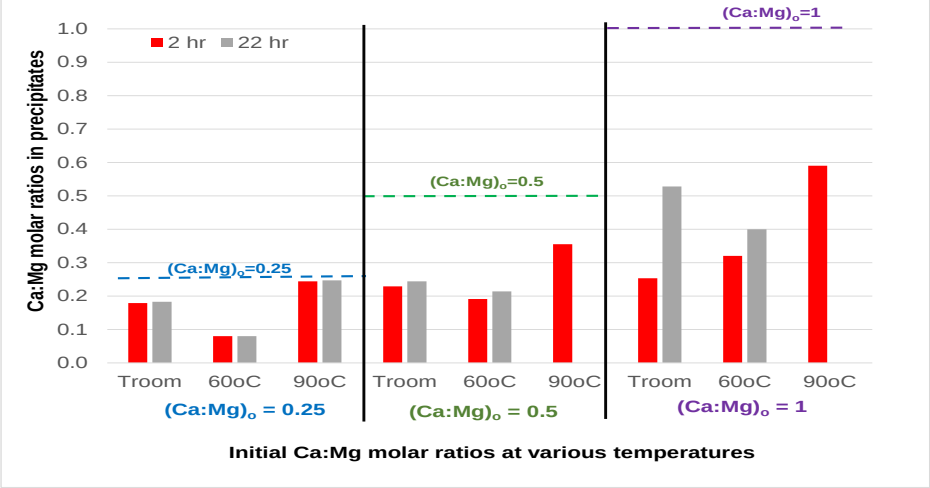

Figure 7: Ca:Mg molar ratios in the precipitates formed in Experiment 5 (940Si:450Mg:187.5Ca) & Experiment 6 (940Si:450Mg:375Ca) & Experiment 7 (940Si:450Mg:750Ca) at various temperatures

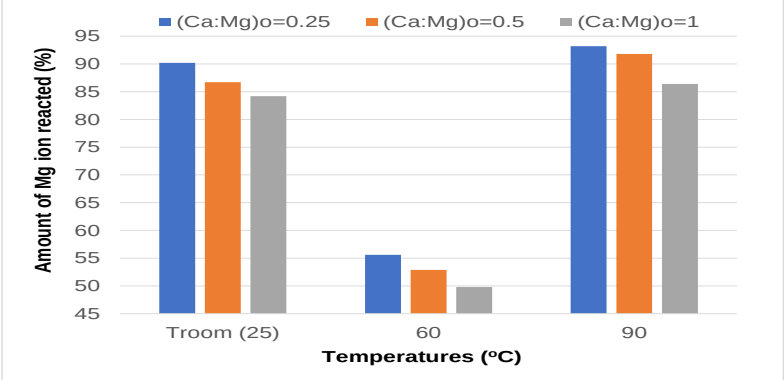

Figure 8: The percentage amount of Mg ion reacted in the presence of various Ca ion concentrations at various temperatures

It was found that the percentage amount of Mg ion reacted decreased as the amount of Ca ion present in the scaling solution was increased. This is true for all temperatures tested as shown in Figure 8. This indicates that the solubility of Mg-silicate increases in the high concentration of Ca ion environment.

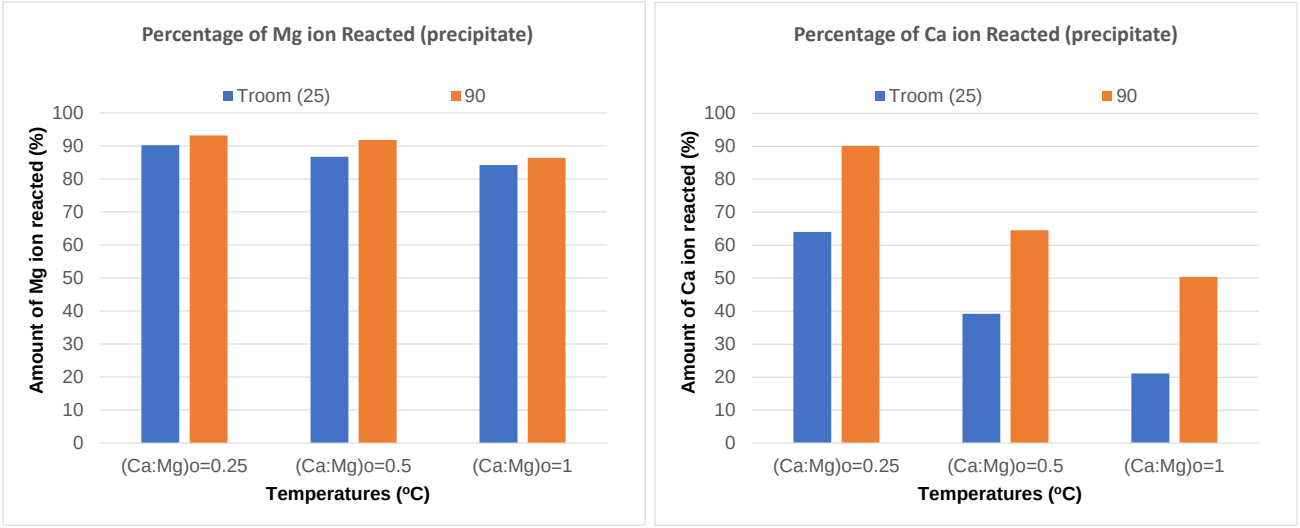

Figure 9: Percentage amount of Mg and Ca ion Reacted at T_{room} and 90°C

Figure 9 shows that more magnesium and calcium are bridging with the silica which occurred at higher temperatures, compared to room temperature. Differences in the amount of magnesium and calcium ions reacted as calculated from the AAS data indicated that different compounds may be produced in the precipitates for each test condition. Hence, temperature certainly affects the types and stoichiometry of the compounds present in the final precipitate.

4.3 XRF Results: Elemental Composition of the Metal-Silicate Scales

XRF data in Figure 10 shows the decrease in the percentage of silica and magnesium concentration in contrast with the increase in the percentage of calcium as the temperature increased from T_{room} to 90°C.

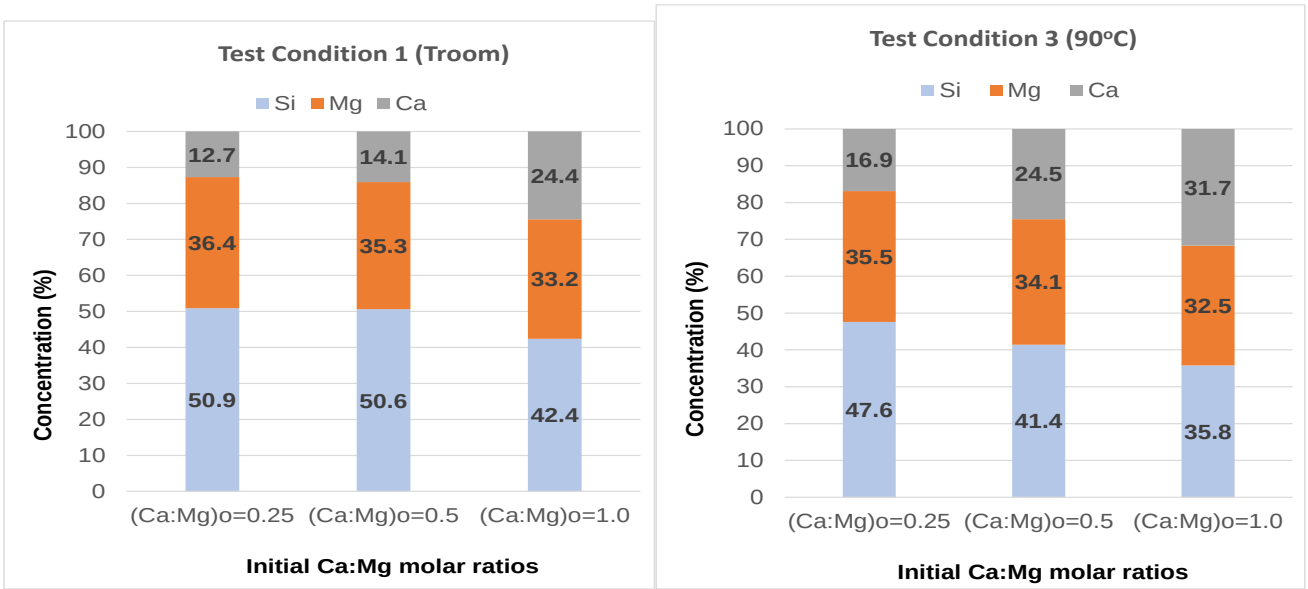

Figure 10: The element concentration analysed by XRF for various $(Ca:Mg)_o$ at various temperatures

This XRF data complemented the AAS analysis that proved silica had a higher tendency to bridge the Mg ion than the Ca ion, and that silica reacted with more Ca ion at high Ca concentrations and higher temperatures.

At high temperature and high Ca concentration (relative to Mg ion), Ca ion has a high tendency to bridge the Si backbone. Hauksson (1995) reported that commonly encountered cations affect solubility in the order of Mg > Ca >Sr> Li> Na >K.

4.4 FTIR Results and Analysis: Materials and Functional Groups Identification

The overlain FTIR spectra of the various silicate precipitates are shown in Figure 11 to Figure 13. Based on the FTIR data in Figure 11, the formation of amorphous silica in the initial silicon concentration mixed brine of 1880ppm and 940ppm was confirmed by the presence of 1738 cm^{-1} band which was in the region of Si-O symmetric bonding. The peaks at 539 cm^{-1}, 527 $cm^{-1,}$ and 1435 cm^{-1} were all related to the Si-O-Si bending and stretching vibration of the silica group (Choudhary et al., 2015). The stretching vibrational modes at 1365 cm^{-1} and 1216 cm^{-1} came from the Si=O bond of the SiO_4 group (Elnahrawy et al., 2015). The infrared spectra peaks at 1092 cm^{-1} and 895 cm^{-1} were in the region of stretching vibration for Si-O symmetric and Si-OH asymmetric bond vibration. The peaks in Figure 11 for both Si concentrations were generally the same; though the intensity was different with the highest intensity being recorded at the higher temperature, T = 90°C.

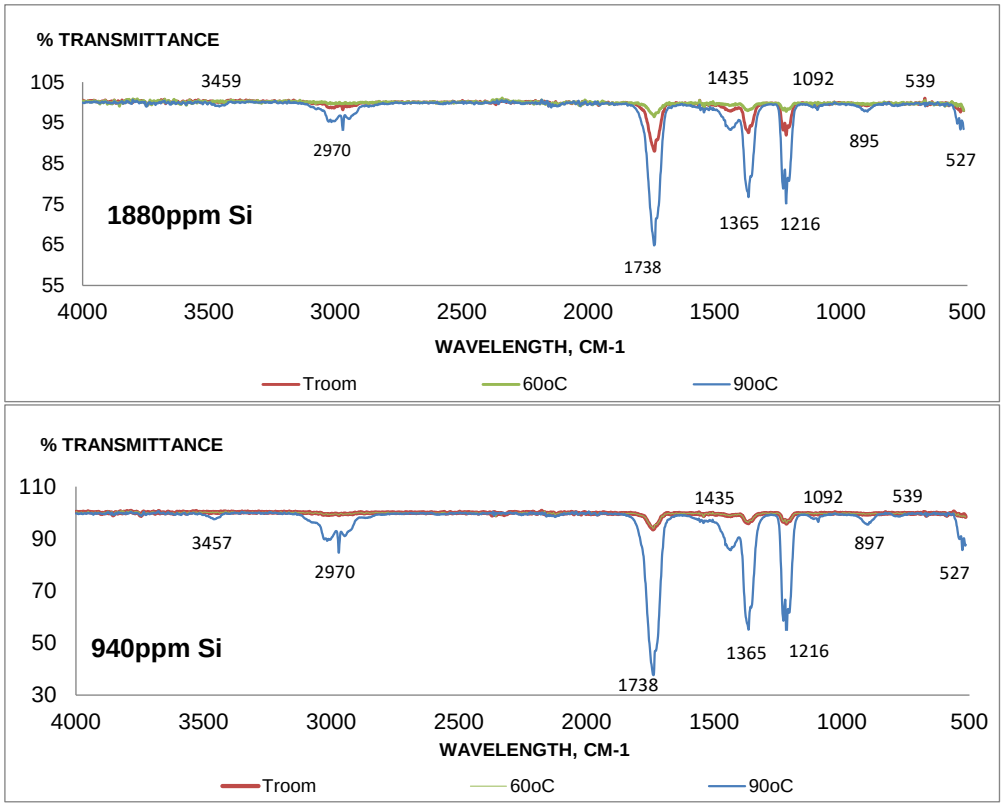

Figure 11: FTIR Spectra for Precipitate Formed in Si-containing Brine only of 1880 ppm Si (Top) and 940ppm Si (Bottom) at Various Temperatures

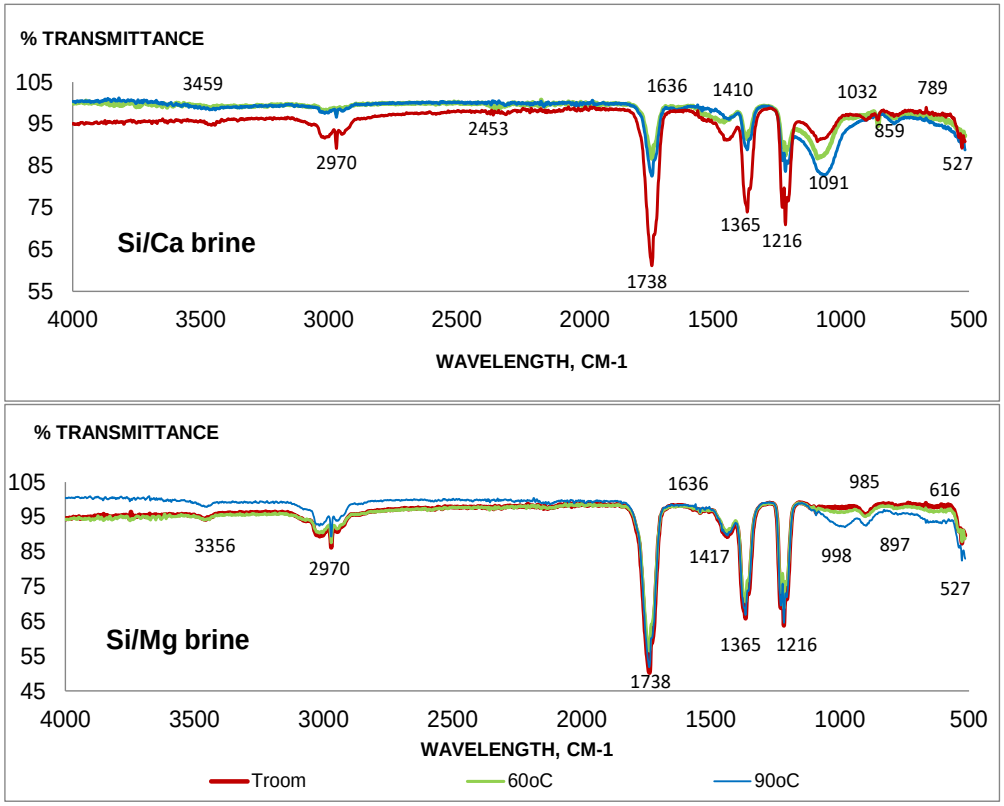

Figure 12: FTIR Spectra for Precipitate Formed in Si/Ca & Si/Mg Scaling Brine of 940Si:900Ca (Top) and 940Si:900Mg (Bottom) at Various Temperatures.

Based on Figure 12, the precipitates formed in the mixed brine of 940Si:900Ca and 940Si:900Mg exhibited the same FTIR peaks with the Si-containing solution at 527 cm^{-1}, 1216 cm^{-1}, 1365 cm^{-1}, 1738 cm^{-1}, 2970 cm^{-1}, and 3457 cm^{-1} to 3459 cm^{-1}. These peaks indicated the formation of amorphous SiO_2 in both scaling brines. The peak that appeared in the 1636 cm^{-1} band in both Si/Ca and Si/Mg scaling solutions belonged to the bending vibration of water molecules (Choudhary et al., 2015).

The peaks observed for the precipitates of the Si/Ca scaling solution as shown in Figure 12 (Top) at 854 cm^{-1} to 859 cm^{-1} and 1410 cm^{-1} belonged to Ca-O-Ca stretching (El-Nahhal et al., 2018). 1065 cm^{-1}, 1032 cm^{-1} peaks showed the symmetric and symmetric stretching of O-Si-O bonding whereas 788 cm^{-1} to 789 cm^{-1} showed Ca-O(Si) (Choudhary et al. (2015). Generally, the same peaks were observed in the scale deposited in the Si/Ca scaling brine environment, although their intensity was different as the temperatures varied from room temperature to 60°C and 90°C, respectively.

A detailed analysis of Si/Mg FTIR spectra in Figure 12 (Bottom) revealed that the peaks belonged to the MgO and Mg-OH bending vibration as observed at 616 cm^{-1} and 1417 cm^{-1} (Ravi & Kaur, 2015). Karakassides et al. (1997, 1999) reported the peaks for Si-O-Si and Si-O-M (where M=Al, Mg, or Fe) were at 950 to 1200 cm^{-1} whereas Jäger et al. (2003) reported that the Si-O stretching vibration shifted from 1111.11 cm^{-1} for the pure SiO_2 to 1030.93 cm^{-1} for $MgSiO_3$ and 975.61 cm^{-1} for $Mg_2.4SiO_{4.4}$. Again, the same peaks were observed in this Si/Mg scaling brine environment although their intensity was different as the temperatures increased from room temperature to 90°C.

A more detailed analysis revealed the intensity of the infrared spectra peaks at 1092 cm^{-1}, which showed that the stretching vibration of Si-O symmetric and Si-OH asymmetric bond vibration in the precipitate deposited from Si-containing brine environment became more obvious in the precipitates deposited in the Si/Ca scaling environment. However, this peak was observed to further shifted to the right at 998 cm^{-1} in the Si/Mg driven precipitates. As we may recall, Si was the only cation presence in the solution that resulted in the IR band, see Figure 11, while the spectra portrayed in Figure 12 was initiated from the cations of Ca or Mg (in addition to the Si); hence, this peak may be used as the fingerprint for SiO_2 or Ca-silicate or Mg-silicate scale.

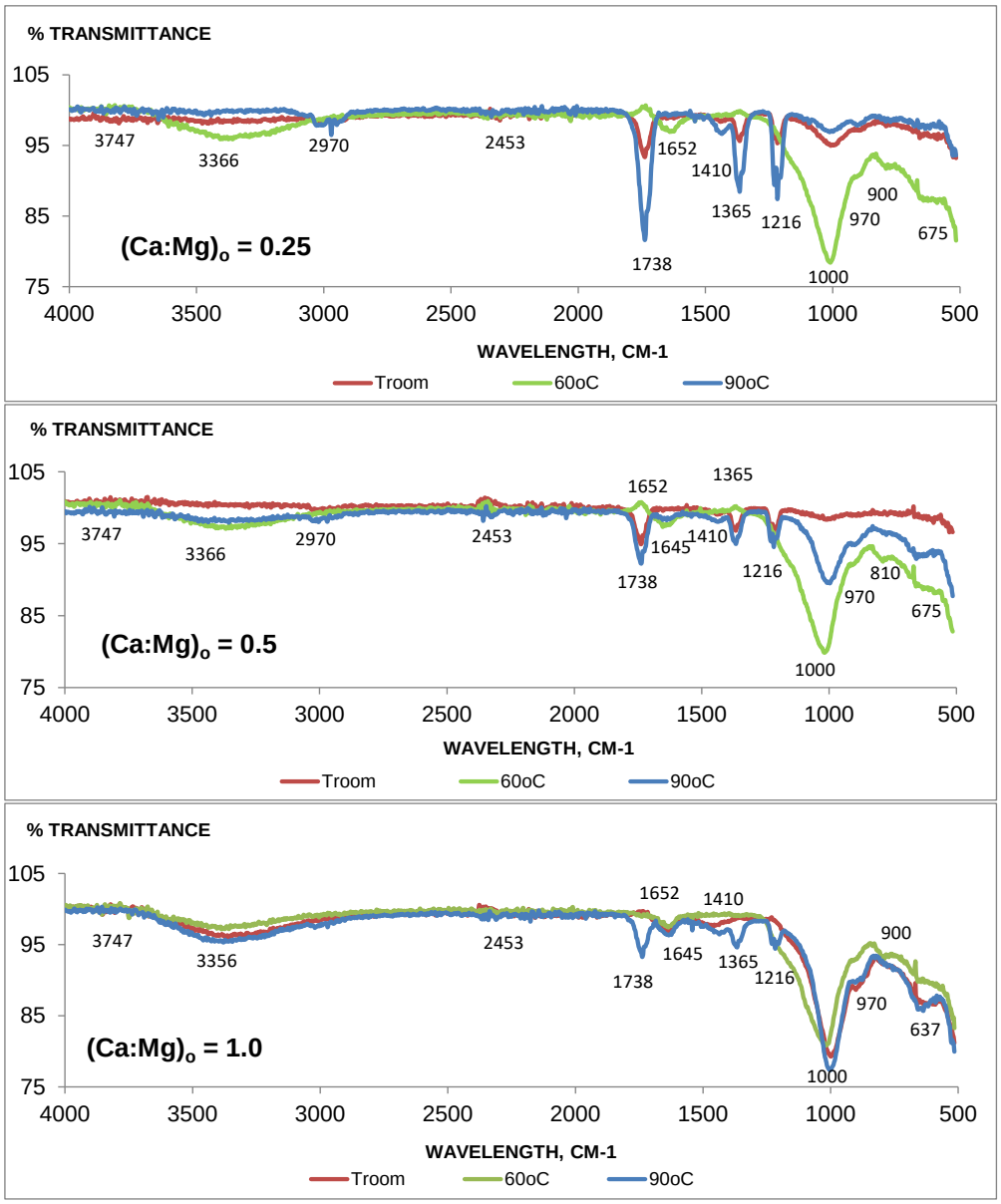

Figure 13: FTIR Spectra for Precipitate Formed in Si/Ca/Mg Scaling Brine of 940Si:450Mg:187.5Ca (Top), 940Si:450Mg:375Ca (Middle) and 940Si:450Mg:750Ca (Top) (Bottom) at Various Temperatures

The FTIR spectrum of three different initial calcium concentrations at various temperatures in Figure 13 shows bands attributed to the Si-O bonding at 1738 cm-1, O-Si-O bonding at 527 cm-1, S=O bonding of SiO_4 group at 1365 cm^{-1} and 1216 cm^{-1} (Ravi & Kaur, 2015). On further analysis, the peak observed at 1092 cm^{-1} indicated the stretching vibration of Si-O symmetric and Si-OH asymmetric bond vibration which moved further to the right at 1000 cm^{-1}. This indicated that the

amorphous silica was more readily bridging the Mg ion than the Ca ion. However, the intensity of the IR spectra in the 500-1000 regions became more obvious as the Ca concentration increased, indicating more Ca ions bridging occurred in the amorphous silica. The overlain IR spectra at various temperatures (for all initial Ca/Mg molar ratios tested) were slightly different especially when the temperature increased to 60°C. This clearly shows that temperature affects the type and morphology of the precipitates.

4.5 XRD Results and Analysis: Crystallographic Structure of the Silica/ Silicate Scale

Figure 14 shows the XRD pattern for Si-only brine for the two concentrations of 1880ppm and 940ppm. An amorphous peak with the equivalent Bragg angle at $2\theta = 21.7^{o}$ was recorded for all temperatures which agreed to Musić et al. (2011) and Liang et al. (2012). These XRD patterns lead to the conclusion that there was a microcrystalline silica scale in the sample containing Si only, Si/Ca, Si/Mg, and Si/Mg/Ca at all temperatures tested. This is proven by the obvious peak (neither humps nor sharp peaks) in all XRD spectra.

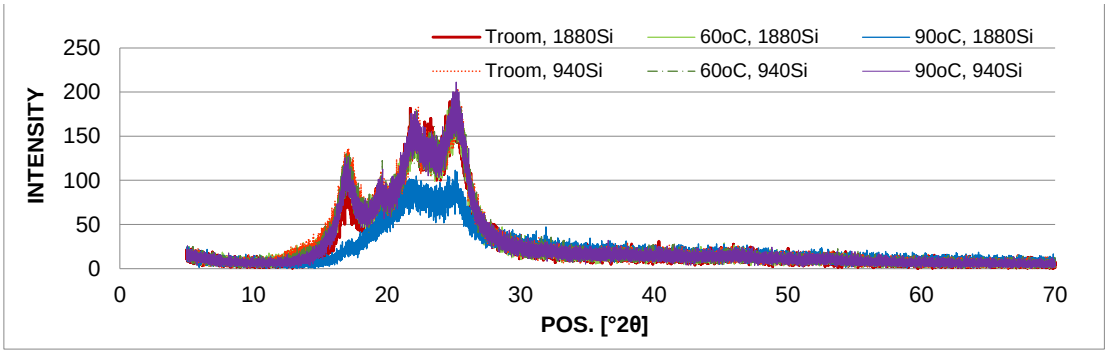

Figure 14: XRD Pattern for Si-only Containing Brine of 1880ppm Si (Top) and 940ppm Si (Bottom) at Various Temperatures

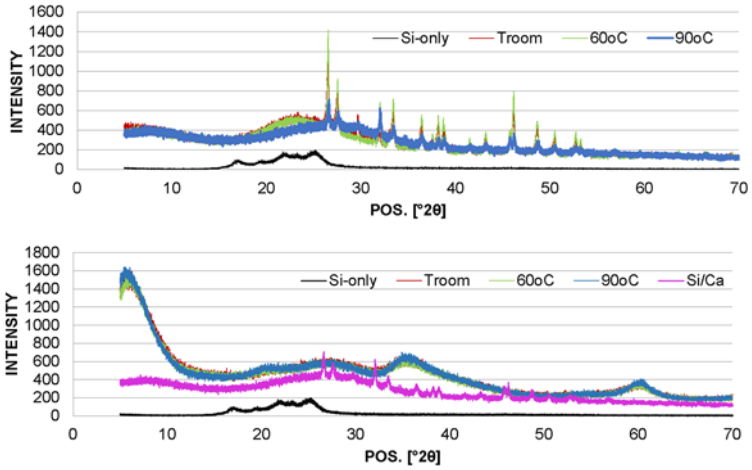

Figure 15: XRD Pattern for Si/Ca (Top) and Si/Mg (Bottom) at Various Temperatures

Figure 15 (Top) shows the dispersion diffraction hump at 23.4° (multiple sharp peaks at 26.5°, 27.5°, 29.7°, 32.0°, 33.4°, 36.4°, 37.5°, 38.2°, 38.7°, 41.5°, 43.2°, 46.1°, 48.6°, 50.4°, 52.7°, and 53.2°) in the XRD patterns for Si/Ca brine, indicating that the synthesis of calcium silicate was of a microcrystalline and amorphous nature at room temperature and 60°C. However, the hump at 23.4°

appeared when the temperature was increased to 90°C, suggesting that calcium silicate produced at 90°C was crystalline.

A detailed analysis of the XRD dispersion pattern for precipitates deposited from the Si/Mg scaling brine revealed two amorphous peaks at 2θ (35.6°) and 2θ (60.1°). These are associated with the formation of magnesium silicate as reported by Zhang et al. (2018). All the amorphous peaks are consistent and can be seen at all temperatures tested suggesting that the magnesium silicates formed are amorphous when deposited at room temperature up to 90°C.

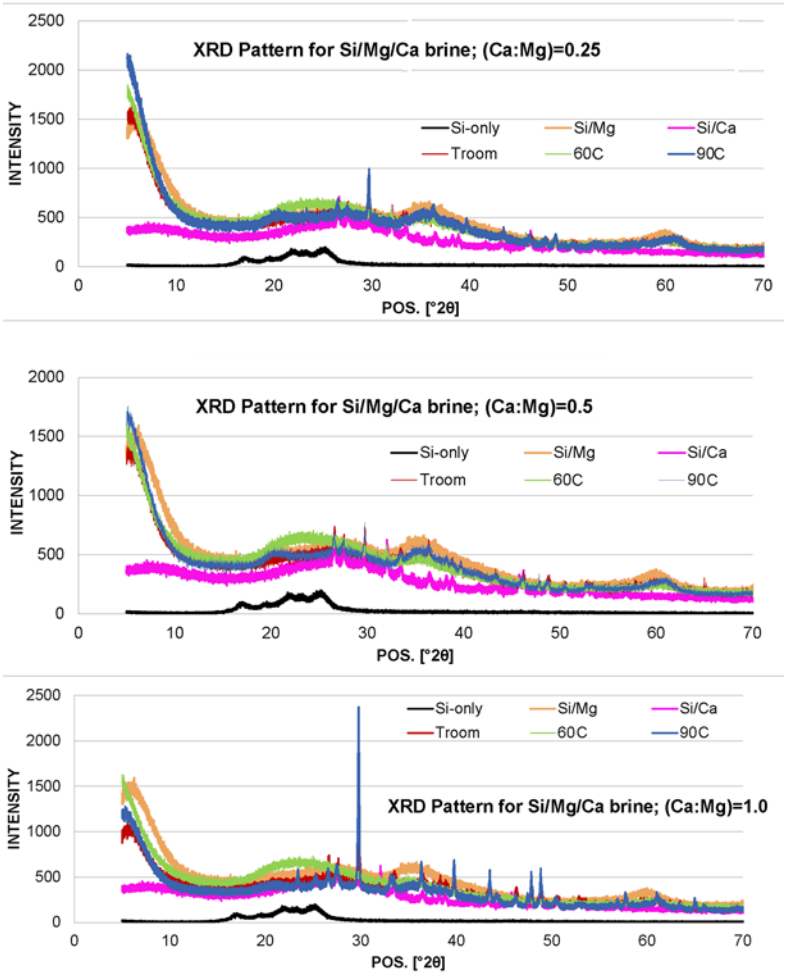

Figure 16: XRD Pattern for Si/Mg/Ca of $(Ca:Mg)_o$=0.25 (Top); $(Ca:Mg)_o$=0.5 (Middle); and $(Ca:Mg)_o$=1.0 (Bottom) at Various Temperatures

Figure 16 (Top) clearly shows that at room temperature, the precipitates deposited from low initial calcium ion i.e. $(Ca:Mg)_o$=0.25, and this case resembled the amorphous magnesium silicate suggesting that amorphous silica has readily bound the Mg ion as compared to Ca ions. However, it started to bind more Ca ions at 90°C as the diffraction peaks shown at various 2θ resembled more crystalline calcium silicate. This observation holds for $(Ca:Mg)_o$=0.5 and $(Ca:Mg)_o$=1.0, see clearly in Figures 16(Middle) and 16(Bottom) respectively. The XRD analysis complemented the AAS, XRF, and FTIR analyses which proved that the amorphous silica scale had a higher tendency to bridge Mg ions more readily at low temperature before it started to bind more Ca ions at a higher temperature and relatively higher Ca ion concentrations.

5 Conclusion

From the study, it can be concluded that the severity, type, and morphology of the silicate scale produced are greatly affected by the temperature of the mixed solution. The evidence can be seen from the different amounts of magnesium and calcium ions reacted as calculated from AAS analysis. It is observed that silicon tends to react with magnesium instead of calcium when both ions are present at the same time. However, at higher concentrations of calcium ions, these ions may bridge with the silica; thus, forming calcium silicate; i.e. the tendency to form calcium silicate scale increases with the increased initial calcium concentration and at higher temperatures. It is also demonstrated that the morphology of the precipitates produced (i.e. whether the silicate is crystalline or amorphous in nature) is highly dependent on the relative ion mixture (and concentration) as well as temperature.

6 Availability of Data and Material

Data can be made available by contacting the corresponding author.

7 Acknowledgment

This work is supported by the Ministry of Higher Education (MOHE) Malaysia and Universiti Teknologi MARA (UiTM), under the Fundamental Research Grant Scheme (grant no 600-IRMI/FRGS 5/3 (411/2019).

8 References

Amjad, Z. & Zuhl, R.W. (2009). *Silica Control in Industrial Water Systems with a New Polymeric Dispersant*. Association of Water Technologies, Inc. Annual Convention & Exposition. Hollywood, Florida, USA.

Babadagli, T. (2007). *Development of mature oil fields - A review. Journal of Petroleum Science and Engineering, 57*(3-4), 221-246. doi:10.1016/j.petrol.2006.10.006

Brown, K. (2011). Thermodynamics and Kinetics of Silica Scaling. *Proceedings International Workshop on Mineral Scaling 2011*, (May): 1-9.

Choudhary, Rajan, Sivasankar Koppala, & Sasikumar Swamiappan. (2015). Bioactivity Studies of Calcium Magnesium Silicate Prepared from Eggshell Waste by Sol-Gel Combustion Synthesis. *Journal of Asian Ceramic Societies, 3*(2), 173-77.

El-Nahhal, I.M., Salem, J.K. & Tabasi, N.S. (2018). Uptake of Curcumin by Supported Metal Oxides (CaO and MgO) Mesoporous Silica Materials. *Journal of Sol-Gel Science and Technology, 87*(3), 647-56.

Elnahrawy, A., Hammad, A.B.A., Turky, G.M., & Elnasharty, M. (2015). Synthesis and Characterization of Hybrid Chitosan/Calcium Silicate Nanocomposite Prepared Using Sol-Gel Method. *International Journal of Advancement in Engineering, Technology and Computer Sciences*, IJAETCS (January).

Gill, J.S. (1998). Silica scale control. *Proc. of the Corrosion 98*, NACE 1998 Paper 226, San Diego, CA.

Gunnarsson, I. & Arno´rsson, S. (2003). Silica scaling: The main obstacle in efficient use of high-temperature geothermal fluids. *International Geothermal Conference*, Reykjavik, Iceland, 3036.

Guo, H., Li, Y., Wang, F., Yu, Z., Chen, Z., Wang, Y., & Gao, X. (2017). ASP Flooding: Theory and Practice Progress in China. *Journal of Chemistry*, 1-18. doi: 10.1155/2017/8509563

Hauksson, T., Thorhallsson, S., Gunnlaugsson, E., & Albertsson, A. (1995). Control of magnesium silicate scaling in district heating systems. *The World Geothermal Congress*.

Jäger, C., Dorschner, J., Mutschke, H., Posch, Th., & Henning, Th. (2003). Steps toward interstellar silicate mineralogy VII. Spectral properties and crystallization behaviour of magnesium silicates produced by the sol-gel method. *Astronomy & Astrophysics*, *408*(1), 193-204.

Jing, G., Tang, S., Li, X., Yu, T., & Gai, Y. (2013). The Scaling Conditions for ASP Flooding Oilfield in the Fourth Plant of Daqing Oilfield. *Journal of Petroleum Exploration & Production Technology*, *3*(3), 175-78.

Karakassides, M.A., Gournis, D. & Petridis, D. (1997). Infrared reflectance study of thermally treated Li- and Cs-montmorillonites. *Clay Minerals*, *45*(5), 649 - 658.

Karakassides, M.A., Gournis, D. & Petridis, D. (1999). An infrared reflectance study of Si-O vibrations in thermally treated alkali-saturated montmorillonites. *Clay Minerals*, *34*(3), 429 - 438. DOI: https://doi.org/10.1180/000985599546334.

Liang, Y. Ouyang, J., Wang, H., Wang, W., Chui, P., & Sun, K. (2012). Synthesis and characterization of core-shell structured SiO2@YVO_4:Yb^{3+}, Er^{3+} microspheres. *Applied Surface Science, 258*(8), 3689-3694.

Mahat, S.Q.A., Saaid, I.M., & Lal, B. (2016). Green Silica Scale Inhibitors for Alkaline-Surfactant-Polymer Flooding : A Review. *Journal of Petroleum Exploration and Production Technology*, *6*(3), 379-85.

Musić, S., Filipović-Vinceković, N., & Sekovanić, L. (2011). Precipitation Of Amorphous SiO_2 Particles And Their Properties. *Braz. J. Chem. Eng.*, *28*(1). https://doi.org/10.1590/S0104-66322011000100011.

Nurxat, N., Gussenov, I. & Tatykhanova, G. (2015). Alkaline / Surfactant / Polymer (ASP) Flooding. (September)

Oddo, E. J., Smith, P. J. & Tomason, B. M. (1991). Analysis of and Solutions to the $CaCO_3$ and $CaSO_4$ Scaling Problems Encountered in Wells Offshore Indonesia. *The 66th Annual Technical Conference and Exhibition of the Society of Petroleum Engineering*, 1-10.

Ravi, S. & Kaur, J. (2015). Characterisation and Mechanoluminescence Studies of $Sr_2MgSi_2O_7$: Eu^{2+}, Dy^{3+}. *Journal of Radiation Research and Applied Sciences*, *8*(2), 201-7.

Sonne, J., Miner, K., & Kerr, S. (2012). Potential for Inhibitor Squeeze Application for Silicate Scale Control in ASP Flood. *Society of Petroleum Engineers - SPE EOR Conference at Oil and Gas West Asia 2012*, OGWA - EOR: Building Towards Sustainable Growth 1: 309-15.

Umar, A.A, & Saaid, I.M. (2013). Silicate Scales Formation during ASP Flooding: A Review. *Research Journal of Applied Sciences, Engineering and Technology*, *6*(9), 1543-1555.

Zhang, T., Zou, J., Wang, B., Wu, Z., Jia, Y., & Cheeseman, C.R. (2018). Characterization of Magnesium Silicate Hydrate (MSH) Gel Formed by Reacting MgO and Silica Fume. *Materials*, *11*(6), 909-923.

Dr. Rozana Azrina Sazali is a Senior Lecturer at the Department of Oil and Gas Engineering, School of Chemical Engineering, College of Engineering, Universiti Teknologi MARA, Malaysia. She got his Ph.D. degree in Petroleum Engineering from Heriot-Watt University, Edinburgh, United Kingdom. Her research focuses on Oilfield Chemistry and Energy Efficiency.

Noor Shamimi Ramli got her Bachelor's Degree in Oil and Gas Engineering from Universiti Teknologi MARA, Malaysia. Her research focuses on Oilfield Chemistry.

Professor Dr.Ken Sorbie is the Cairn Energy Professor of Petroleum Engineering at Heriot-Watt University, Edinburgh, United Kingdom. He has a first degree in Chemistry from Strathclyde University and a DPhil in Theoretical Chemistry/Applied Mathematics from the University of Sussex. His research is in three main areas: (i) the fundamentals of Multiphase Flow through Porous Media, (ii) Oilfield Chemistry, particularly Mineral Scale Formation and Control, and (iii) Enhanced Oil Recovery (EOR) both by Gas Injection (WAG) and Chemical Methods such as Injection of Polymer, and Surfactant.

Dr. Lorraine Boak is a Senior Research Fellow/Laboratory Manager in the Flow Assurance and Scale Team (FAST) and the associated Research and Consultancy activity (FASTrac) in the Institute of Petroleum Engineering at Heriot-Watt University. She holds a BSc (Hons) in Chemistry and both MPhil and PhD degrees in Petroleum Engineering, all from Heriot-Watt University. Her research interests include Oilfield Scale Surface Nucleation and Growth Inhibition, and Chemical Analysis Techniques – ICP and Wet Chemical Methods.